JOURNAL OF AGRICULTURAL AND FOOD CHEMISTRY

Article

pubs.acs.org/JAFC

Optical Detection of λ-Cyhalothrin by Core−Shell Fluorescent Molecularly Imprinted Polymers in Chinese Spirits

Jixiang Wang,[†] Lin Gao,[†] Donglai Han,[§,#] Jianming Pan,[†] Hao Qiu,[†] Hongji Li,[†] Xiao Wei,[‡] Jiangdong Dai,[†,‡] Jinghai Yang,[#] Hui Yao,[†] and Yongsheng Yan*[,†]

[†]School of Chemistry and Chemical Engineering and [‡]School of Material Science and Engineering, Jiangsu University, Zhenjiang 212013, People's Republic of China

[§]Changchun Institute of Optics, Fine Mechanics and Physics, Chinese Academy of Sciences, Changchun 130033, People's Republic of China

[#]Key Laboratory of Functional Materials Physics and Chemistry of the Ministry of Education, Jilin Normal University, Siping 136000, People's Republic of China

Supporting Information

ABSTRACT: In this study, fluorescent molecularly imprinted polymers (FMIPs), which were for the selective recognition and fluorescence detection of λ-cyhalothrin (LC), were synthesized via fluorescein 5(6)-isothiocyanate (FITC) and 3-aminopropyltriethoxysilane (APTS)/SiO_2 particles. The SiO_2@FITC-APTS@MIPs were characterized by Fourier transform infrared (FT-IR), UV−vis spectrophotometer (UV−vis), fluorescence spectrophotometer, thermogravimetric analysis (TGA), confocal laser scanning microscope (CLSM), scanning electron microscopy (SEM), and transmission electron microscopy (TEM). The as-synthesized SiO_2@FITC-APTS@MIPs with an imprinted polymer film (thickness was about 100 nm) was demonstrated to be spherically shaped and had good monodispersity, high fluorescence intensity, and good selective recognition. Using fluorescence quenching as the detection tool, the largest fluorescence quenching efficiency ($F_0/F - 1$) of SiO_2@FITC-APTS@MIPs is close to 2.5 when the concentration of the LC is 1.0 μM L^{-1}. In addition, a linear relationship ($F_0/F - 1 = 0.0162C + 0.0272$) could be obtained covering a wide concentration range of 0−60 nM L^{-1} with a correlation coefficient of 0.9968 described by the Stern−Volmer equation. Moreover, the limit of detection (LOD) of the SiO_2@FITC-APTS@MIPs was 9.17 nM L^{-1}. The experiment results of practical detection revealed that the SiO_2@FITC-APTS@MIPs as an attractive recognition element was satisfactory for the determination of LC in Chinese spirits. Therefore, this study demonstrated the potential of SiO_2@FITC-APTS@MIPs for the recognition and detection of LC in food.

KEYWORDS: *λ-cyhalothrin, molecular imprinted polymer, fluorescence detection, selective recognition, precipitation polymerization*

INTRODUCTION

Pyrethroid, which has the advantages of high efficiency, low toxicity, and biodegradability, is a kind of broad pesticide, and it can be used for pest prevention and management. It is used mainly to prevent plant diseases and insect pests of tea, vegetables, chrysanthemum, and tobacco, as well as parasites of the aquaculture industry.[1] Due to its low dosage and concentration, it is not only safe to humans and livestock but also has few side effects on the environment. Therefore, it has been a pesticide product promoted and popularized by the national Chinese government. According to some statistics, pyrethroid insecticides have been widely used on farmlands. The proportion of pyrethroid insecticides is about 20% of the insecticide market, and they account for 25% of insecticide using square. So far, over 50 kinds of pyrethroids have been commercialized.[2] Generally, the long-term and repeated use of pyrethroid insecticides and their residue would gather in water products, such as fish and some beneficial insects. Then the pyrethroid insecticides would do harm to them, and at the same time it would also lead to drug resistance of insect pest. With the gathering of pyrethroid insecticides in water organisms, it will do harm to humans and livestock via food chain and many other methods.[3] Accordingly, the maximum residue limits for pyrethroid insecticides are strictly set by governments all over the world;[4] for example, the maximum residue limit for pyrethroid residues set by the U.S. Environment Protection Agency (EPA) is not more than 0.05 μg g^{-1}.[5] In recent years, direct methods for the determination of pyrethroids are mainly based on gas chromatography (GC),[6−9] high-performance liquid chromatography (HPLC),[10] or thin-layer chromatography (TLC).[11,12] Argauer et al.[13] and Ramesh and Balasubramanian[14] determined pyrethroid insecticides with solid-phase extraction (SPE)−GC methodology. Huang et al.[15] separated λ-cyhalothrin (LC) with a double capillary column (HP-5, DB1701) by GC and detected LC by electron capture detector. Deme et al.[16] determined pyrethroid insecticides with a modified dispersive solid-phase extraction methodology and gas chromatography−negative chemical ion source−mass spectrometry (GC-NCI-MS). The methodology was successfully applied in the rapid analysis of many kinds of pyrethroids in cooking oil. Esteve-Turrillas et al.[17] extracted

Received: September 17, 2014
Revised: January 21, 2015
Accepted: January 29, 2015
Published: January 29, 2015

DOI: 10.1021/jf5043823
J. Agric. Food Chem. 2015, 63, 2392−2399

Table 1. Different Methods of Detection Pyrethroids

methodology	detection limit	detection rate (%)	advantages	disadvantages
this method	9.17−60 nM L^{-1}	61.4−106.2	high sensitivity, simplicity, speed, convenience, efficiency	immaturity, boundedness
Huang et al.[15]	2.1−6.9 ng kg^{-1}	73.4−120.1	accuracy, high sensitivity	multistep, time-consuming, expensive instruments
Deme et al.[16]	0.01−1 μg kg^{-1}	62−110	accuracy, high sensitivity	multistep, complexity, time-consuming, expensive instruments,
Esteve-Turrillas et al.[17]	0.08−5.4 μg kg^{-1}	84−120	accuracy, high sensitivity	multistep, complexity, time-consuming, expensive instruments
Ma and Chen[34]	3.5 ng kg^{-1}	82.4−101.7	accuracy, high sensitivity	multistep, complexity, time-consuming, inaccuracy
Song et al.[37]	5−10 μM L^{-1}	97.8−103.5	convenience, efficiency, simplicity	time-consuming, boundedness, complexity, immaturity

pyrethroids from soil with microwave-aided extraction (MAE) methodology. Although such methods are quite accurate, they depend on multistep sample cleanup procedures and result in relatively expensive and time-consuming processes. Thus, the exploitation of novel functional materials for the simple, rapid, and highly sensitive detection of trace pyrethroid insecticides remains a challenge, especially in complicated sample matrices.

A promising way to achieve the tailored selective detection of analytes is to use molecularly imprinted polymers (MIPs). Because the MIPs can be easily prepared with low cost, in addition to their greater stability, the molecularly imprinted materials will attract more and more people.[18−24] In our research group, Pan and co-workers have synthesized molecularly imprinted polymers based on magnetic halloysite nanotube composites with selective recognition of 2,4,6-trichlorophenol.[25] Xu and co-workers synthesized thermally responsive magnetic molecularly imprinted polymers for selective removal of antibiotics from aqueous solution.[26] Obviously, compared with the traditional separation−enrichment method, MIPs with selective recognition ability can separate the target molecule conveniently and effectively, excluding the influence of any other structural analogues. Moreover, the method to prepare MIPs is simple. Also, MIPs, with good reproducibility, can be stored easily.[27−29] The excellent performance of molecularly imprinted polymers allows them to be widely used in many fields.[30−32] Shi et al.[33] concentrated pyrethroid selectivity from aquaculture water with molecularly imprinted solid phase extraction methodology and detected pyrethroid with GC. Ma and Chen[34] prepared a magnetic surface molecularly imprinted polymer based on carbon nanotube, which adsorbed LC selectively. However, as to the level of molecular imprinting technique, it is still a challenge for us to find a more convenient and effective way to detect pyrethroid pesticide residues in the environment.

The fluorescence detection method is efficient, simple, and sensitive. It has great potential in the field of analyzing samples quickly. Compared with HPLC, it has advantages in solvent consumption, sample pretreatment, and test time. We can design an experiment to adapt the molecular imprinting technology to fluorescence detection, to take advantage of the recognition and capture ability of MIPs to make target molecules be adsorbed on MIPs selectively, in order that they can be separated with interfering substances, and then the fluorescence analyzer can be used to detect fluorescence. For the reason that it contains fluorescent nanomaterials during the synthesizing process of molecularly imprinted polymerization, the fluorescence intensity will quench after the reaction of target molecules and MIPs.[35] Zhao et al. have synthesized composite quantum dots molecularly imprinted polymer (QDs@MIP) nanospheres for specific recognition and direct fluorescent quantification of pesticides in aqueous media.[36] Song et al.[37] prepared porous silica fluorescent nanospheres recognizing LC in aqueous media efficiently. We make the comparison of this method and other methods in Table 1. As shown in the table, the method of detection of LC has some advantages compared with the others. This method not only has the advantages of high sensitivity, simplicity, efficiency, speed, and convenience but also could deal with complex samples. The interference of coexisting substance in specimen material can be eliminated by this coupling technology, and the selectivity of molecular imprinting can be combined with the high sensitivity of fluorescence detection. As a result, we get a new detection and analysis method.

In this study, fluorescent molecularly imprinted polymers (SiO_2@FITC-APTS@MIPs) were proposed for the analysis of LC based on the LC-resulted fluorescence quenching of the fluorescent dye anchored on the MIP polymer, which was covalently coated on the surface of SiO_2 via a surface molecular imprinting process. We chose Chinese spirit as a practical sample, a kind of distilling liquor unique to China. Chinese spirit is a popular drink in China for its special aroma. The main raw material of Chinese spirit is grain. However, pyrethroid is a kind of broad-spectrum insecticide for these agricultural products. Therefore, not only can the Chinese spirit as a sample reveal the detection levels of SiO_2@FITC-APTS@MIPs in complex samples but also the SiO_2@FITC-APTS@MIPs can be a steppingstone to detect additional practical samples in the future. On the whole, through the experiment of the fluorescence detection of LC in Chinese spirits, we can see that the SiO_2@FITC-APTS@MIPs have a broad prospect in the food safety analysis field.

EXPERIMENTAL PROCEDURES

Materials. Tetraethyl orthosilicate (TEOS, AR), divinylbenzene (DVB, AR), and fluorescein 5(6)-isothiocyanate (FITC, AR) were all purchased from Aladdin Reagent Co., Ltd. (Shanghai, China). 3-Aminopropyltriethoxysilane (APTS, AR) was purchased from Energy Chemical (Shanghai, China). Acrylamide (AM, AR), acetonitrile, and ammonium hydroxide were all purchased from Sinopharm Chemical Reagent Co., Ltd. (Shanghai, China). 2,2′-Azobis(isobutyronitrile) (AIBN, AR) was obtained from Tianjin Guangfu Fine Chemical Research Institute (Tianjin, China). All of the pyrethroid pesticides, LC, β-cyfluthrin (BC), esfenvalerate (FE), and bifenthrin (BI), were obtained from Yingtianyi Standard Sample Co. (Beijing, China), and the corresponding chemical structures of the pyrethroids are displayed in Figure 5. Doubly distilled water was used for cleaning processes.

Instrument. Infrared spectra (4000−400 cm^{-1}) were recorded on a Nicolet NEXUS-470 FT-IR apparatus (USA). The morphologies of SiO_2@FITC-APTS@MIPs/SiO_2@FITC-APTS@NIPs were observed by a scanning electron microscope (SEM, JEOL, JSM-7001F) and a

DOI: 10.1021/jf5043823
J. Agric. Food Chem. 2015, 63, 2392−2399

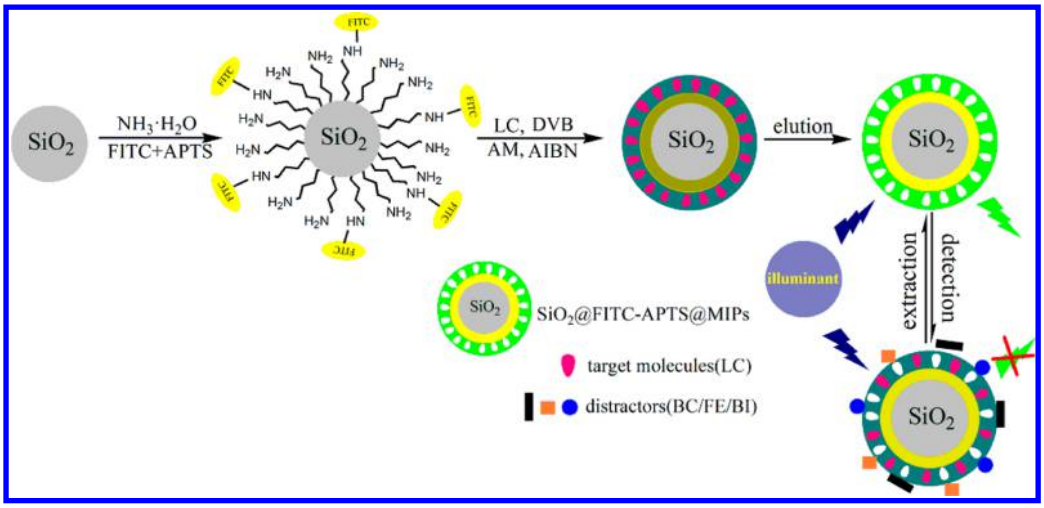

Figure 1. Schematic illustration for the preparation of SiO_2@FITC-APTS@MIPs.

transmission electron microscope (TEM, JEOL, JEM-2100). Fluorescence intensity was measured by using a Cary Eclipse fluorescence spectrophotometer (Varian, USA). UV−vis adsorption spectra were obtained with a UV−vis spectrophotometer (UV-2450, Shimadzu, Japan). Laser confocal microscopy images of SiO_2@FITC-APTS@MIPs samples were observed using a TCS SP5 II confocal microscope (Leica, Germany) with a 488 nm solid state laser light source. Transient fluorescence spectra were measured on a QuantaMaster 40 spectrofluorometer (Photon Technology International, USA). TGA of the samples was performed for powder samples (about 10 mg) using a Diamond TG/DTA instruments (PerkinElmer, USA) under a nitrogen atmosphere up to 1000 °C with a heating rate of 10 °C min^{-1}.

Preparation of SiO_2 and SiO_2@FITC-APTS. Silica has been widely used as substrate material due to its chemical stability and the property of easy modification.[38] First, SiO_2 beads were prepared according to the stöver process.[39,40] Typically, 2.0 mL of $NH_3{\cdot}H_2O$ was dissolved in 25 mL of ethanol and 25 mL of double-distilled water in a 100 mL round-bottom flask by sonication for 15 min. Then, 2.0 mL of TEOS was slowly added into the flask sequentially. The mixture was allowed to react for 24 h at room temperature under a continuous stirring of 1000 rpm. The resulting product was separated from the solvent by centrifuge and washed rotationally by ethanol and double-distilled water several times.

Typically, 40 mg of FITC was dissolved in 2.0 mL of APTS in a 10 mL test tube for 48 h in darkness at room temperature under continuous stirring of 800 rpm first. The reaction formula is shown in Figure S1 in the Supporting Information. After the reaction for 24 h, we obtained a FITC-APTS mixture.[41] Then SiO_2 beads was scattered in 100 mL of ethanol by sonication in a 250 mL brown round-bottom flask, and 5.0 mL of $NH_3{\cdot}H_2O$ and 30 mL of double-distilled water were added into the flask. Then the mixture was slowly added into the flask sequentially and allowed to react for 24 h in darkness at room temperature under continuous stirring of 1000 rpm. The resulting SiO_2@FITC-APTS was separated from the solvent by centrifuge and was repeatedly washed.

Synthesis of SiO_2@FITC-APTS@MIPs and SiO_2@FITC-APTS@NIPs. The synthesis of SiO_2@FITC-APTS@MIPs via a multistep precipitation polymerization procedure is illustrated in Figure 1. The first and second steps were narrated in the above. The third step was to prepare the preassemble solution. Typically, LC (0.50 g, 1.0 mmol) and AM (0.2840 g, 4.0 mmol) were dissolved with 20 mL of acetonitrile in a 50 mL beaker under the dark environment for 1.0 h. Then 200 mg of SiO_2@FITC-APTS beads was added into a 250 mL brown round-bottom flask and scattered in 70 mL of acetonitrile by sonication for 1.0 h. After this, the mixture (LC and AM) was poured into the flask, and 0.8 mL of DVB was added into the flask at the same time. The mixture was degassed in an ultrasonic bath for 10 min and sparged with oxygen-free nitrogen for 10 min. Then, the flask was submerged in a thermostatically controlled oil bath, which was in stirring condition, and the stirring rate was 1200 rpm. After the temperature was increased from room temperature to 60 °C within 30 min, free radical initiator AIBN (about 0.02 g) was added into the flask, and then the temperature was maintained at 60 °C for a further 24 h. After the reaction, the SiO_2@FITC-APTS@MIPs beads were collected from the reaction medium by centrifuge, and the product was rinsed several times with ethanol and double-distilled water. After that, the beads were eluted with 100 mL of acetic acid/methanol (10:90, v/v) to remove LC templates by Soxhlet extractor. Finally, after 5 days of elution, the product SiO_2@FITC-APTS@MIPs were obtained, which were dried under vacuum for 12 h at 40 °C. In principle, the methods of preparing SiO_2@FITC-APTS@NIP beads and SiO_2@FITC-APTS@MIPs were the same, the only difference being that the former lacked the LC template.

RESULTS AND DISCUSSION

Characterization of SiO_2@FITC-APTS@MIPs and SiO_2@FITC-APTS@NIPs. The products of SiO_2, SiO_2@FITC-APTS, and SiO_2@FITC-APTS@MIPs were investigated by FT-IR spectroscopy (Supporting Information, Figure S2). SiO_2 (Figure S2a) spheres displayed the characteristic signals of Si−O at 473 and 803 cm^{-1}, and they were attributed to symmetric stretching vibration and bending vibration, respectively. The strong and broad peak around 1103 cm^{-1} indicated Si−O−Si asymmetric stretching. These results suggested that the tetraethyl orthosilicate successfully condensed into silicon dioxide by hydrolysis. Compared with the infrared data of pure SiO_2, the SiO_2@FITC-APTS (Figure S2b) displayed the characteristic peak of amino groups at 1403 cm^{-1}.[42] The presence of bands around 2926 cm^{-1} suggested the aliphatic C−H stretching.[43] These facts showed the presence of amine ligands on the surface of SiO_2. As shown in Figure S2c, para-substituted benzene surface deformation vibration was about 832 cm^{-1}, meta-substituted benzene surface deformation vibration was about 712 cm^{-1}, and 794 and 900 cm^{-1} were the characteristic peaks of divinylbenzene. The characteristic peaks of the benzene ring frame vibration at about 1606 cm^{-1} and C═O stretching vibration of amide at 1683 cm^{-1} indicated that the MIPs layer had been successfully compounded on the surface of SiO_2@FITC-APTS.

To ascertain the synthesizing of materials further, UV−vis spectra of SiO_2@FITC-APTS@MIPs, SiO_2@FITC-APTS, FITC-APTS, APTS, FITC, and SiO_2 were measured as

DOI: 10.1021/jf5043823
J. Agric. Food Chem. 2015, 63, 2392−2399

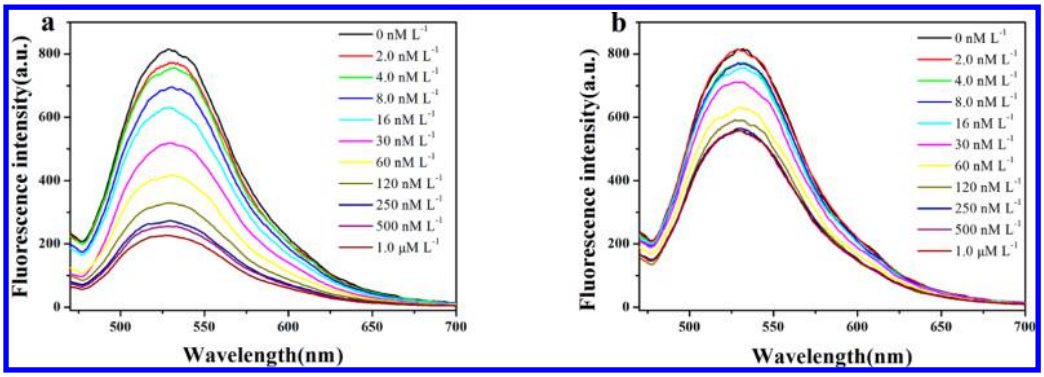

Figure 2. Response of SiO_2@FITC-APTS@MIPs (a) and SiO_2@FITC-APTS@NIPs (b) to LC in the concentration range from 0 to 1.0 μM L^{-1}.

shown in Figure S3 in the Supporting Information. The figure showed that pure SiO_2 (purple) and APTS (green) almost have no visible absorption peaks. The solution of FITC (yellow) displayed two visible absorption peaks at 455 and 485 nm, whereas the FITC−APTS conjugates (blue) showed only one visible absorbance at 502 nm, indicating that a strong interaction occurred between APTS and FITC molecules. In the meantime, the dispersive liquid of SiO_2@FITC-APTS (red) showed nearly a visible absorption peak at 505 nm. The solution of SiO_2@FITC-APTS@MIPs (black) showed a strong absorption peak at 505 nm. From the above phenomenon, we found that the FITC−APTS conjugates, directly and successfully, grafted on the surface of SiO_2 by the means of APTS condensation.

The SiO_2@FITC-APTS@MIPs (black) dispersive liquid displayed the visible absorption peak of dye FITC with the λ_{max} at 506 nm, whereas the pure SiO_2 showed scarcely any visible absorption as indicated in Figure S4 of the Supporting Information. The fluorescence spectra of SiO_2@FITC-APTS@MIPs (blue) dispersive liquid displayed a green fluorescence emission with λ_{max} at 531 nm (excited at 450 nm), which is identical to the emission spectra of the dye FITC.

The size and shape of SiO_2 and SiO_2@FITC-APTS@MIPs were examined by SEM and TEM techniques. The SEM and TEM images of SiO_2 beads are shown in Figure 5a,c. It can be observed that the diameter of pure SiO_2 was about 300 nm. It can be seen that the pure SiO_2 was dispersed fully before polymerization; that is to say, it had the good monodispersity. The size and shape of SiO_2@FITC-APTS@MIPs are shown in Figure 5b,d. After being coated with FITC−APTS and MIPs, the diameter of the SiO_2@FITC-APTS@MIPs increased to about 500 nm, and the grain size was increased about 100 nm. As shown in the inset of Figure 5d, it was clearly observed that the product of SiO_2@FITC-APTS@MIPs beads had an approximately spherical shape and good monodispersity. It is observed that the product of SiO_2@FITC-APTS@MIPs not only keeps the spherical morphology but also still has good monodispersity after polymerization. On the whole, it was confirmed that the SiO_2@FITC-APTS@MIPs beads with core−shell structure had been successfully prepared.

The fluorescent images of SiO_2@FITC-APTS and SiO_2@FITC-APTS@MIPs were observed by confocal laser scanning microscope. Excitation wavelength and emission wavelength were 488 and 525 nm, respectively. Apparently, SiO_2@FITC-APTS@MIPs had strong fluorescence emission. As can be seen from the diagram, the monodispersity of SiO_2@FITC-APTS (a) and SiO_2@FITC-APTS@MIPs (b) did not change greatly before or after aggregation. The molecularly imprinted polymer still had the better monodispersity, and there is no serious reunion, which contributes to detection of the target molecule.

Figure S7 of the Supporting Information shows the TGA of SiO_2@FITC-APTS@MIPs and SiO_2@FITC-APTS@NIPs. It can be observed that the weight losses of SiO_2@FITC-APTS@MIPs and SiO_2@FITC-APTS@NIPs before 900 °C were ∼71.52 and ∼71.91%, respectively. The slight weight difference may be attributed to crystal water. The whole thermogravimetric process could be divided roughly into three stages. First, the temperature was before 100 °C, due to the loss interior water of crystallization. Second, the temperature was started at 350−500 °C, and weight losses of SiO_2@FITC-APTS@MIPs and SiO_2@FITC-APTS@NIPs were about 56.40 and 57.12%, respectively. The second weight loss stage can be ascribed to the polymerization of organic matter decomposition. The third weight loss stage started at 500−920 °C, during which the weight losses of SiO_2@FITC-APTS@MIPs and SiO_2@FITC-APTS@NIPs were 15.12 and 14.79%, respectively. This might be the reason for thermal decomposition of the modification of FITC-APTS. We could draw the conclusions that, first, the curves of imprinting and nonimprinting are almost the same. Second, polymers were grafted onto the surface of SiO_2 particles successfully, and the amounts of loss and use were equal. Finally, better temperature resistance of obtained products proved that thermal decomposition at room temperature does not readily occur.

Fluorescence Detection of SiO_2@FITC-APTS@MIPs Beads. All luminescence experiments were carried out at room temperature. The fluorescence spectrophotometer was used to monitor the fluorescence intensity of different molecularly imprinted polymers with the excitation wavelength of 450 nm. The samples of SiO_2@FITC-APTS@MIPs beads (50 mg) were dispersed in 100 mL alcohol solutions, which were prepared for spectrum measurement. Afterward, we prepared LC solution of different concentration ranges (0−1.0 μM L^{-1}). Then 5.0 mL of the sample solutions was poured into various concentrations of the 5.0 mL LC solution. Before spectrum measurement, the mixture of samples solution was stirred thoroughly. The fluorescence quenching efficiency of the SiO_2@FITC-APTS@MIPs beads with LC was calculated by Stern−Volmer equation, and the linear relationship could be described by $(F_0/F - 1)$ versus the concentration (nM L^{-1}). The same procedure was performed for the SiO_2@FITC-APTS@NIPs.

From the data in Figure 2a, it can be seen that with the increase of concentration of LC, the fluorescence intensity became weaker and weaker, and the reduced degree of fluorescence intensity in SiO_2@FITC-APTS@MIPs was

DOI: 10.1021/jf5043823
J. Agric. Food Chem. 2015, 63, 2392−2399

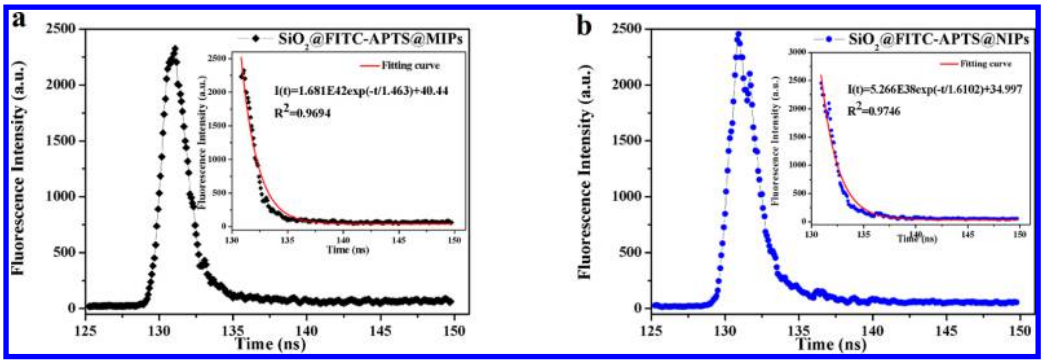

Figure 3. Transient fluorescence spectra of SiO_2@FITC-APTS@MIPs (a) and SiO_2@FITC-APTS@NIPs (b), for which the excitation wavelengths are 450 nm. Time-resolved fluorescence curves SiO_2@FITC-APTS@MIPs and SiO_2@FITC-APTS@NIPs are illustrated.

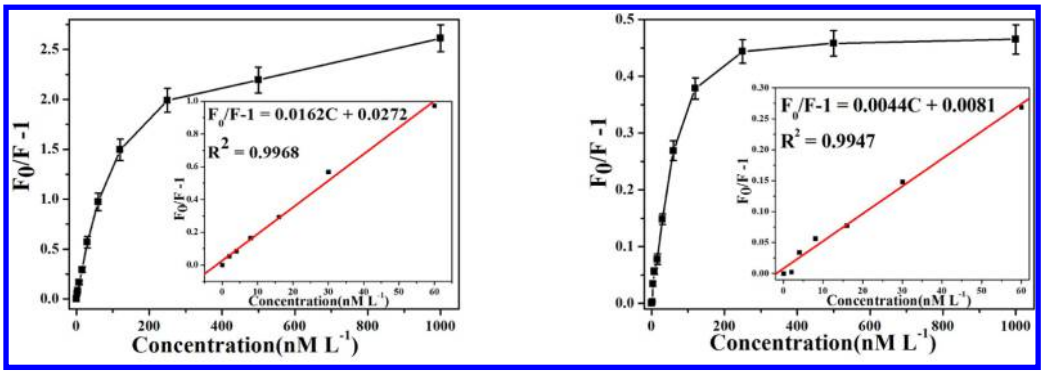

Figure 4. Fluorescence quenching efficiency changed according to LC concentration. (Insets) Linear equations of SiO_2@FITC-APTS@MIPs (a, left) and SiO_2@FITC-APTS@NIPs (b, right).

notably higher than that of the SiO_2@FITC-APTS@NIPs (Figure 2b). Therefore, we found that SiO_2@FITC-APTS@MIPs could detect the LC by fluorescence quenching. However, when the concentration of LC was between 250 and 1000 nM L^{-1}, the fluorescence intensity change was no longer apparent. As shown in Figure 2b, the fluorescence intensity changed, but it was of small amplitude along with the concentration of LC increasing. The fluorescence intensities of the SiO_2@FITC-APTS@MIPs and SiO_2@FITC-APTS@NIPs were important data to evaluate the selectivity and sensitivity of the materials obtained. It was illustrated that the spatial adsorption sites could be incorporated into the SiO_2@FITC-APTS@MIPs matrix, but a slightly in SiO_2@FITC-APTS@NIPs. In addition, it was also confirmed that the SiO_2@FITC-APTS@MIPs beads had been produced successfully.

The transient fluorescence spectra of SiO_2@FITC-APTS@MIPs and SiO_2@FITC-APTS@NIPs are displayed in Figure 3. The time-resolved fluorescence curves are illustrated in Figures. Decay in the fluorescence intensity (I) with time (t) was fitted by an exponential function

$$I(t) = A \exp(-t/\tau)$$

where τ is the lifetime and A is the amplitude.

As can be seen from Figure 3, the obvious fluorescence decay was found clearly illustrated. The two decay curves were fitted by exponential function. The nolinear equations of SiO_2@FITC-APTS@MIPs (Figure 3a) and NIPs (Figure 3b) were $I(t)$ = 1.681E42 exp($-t$/1.463) + 40.44 and $I(t)$ = 5.266E38 exp($-t$/1.6102) + 34.997, and the corresponding correlation coefficients (R^2) were R^2 = 0.9694 and R^2 = 0.9746, respectively. From the equations, we found that the lifetimes of SiO_2@FITC-APTS@MIPs and NIPs are τ = 1.463 ns and τ_0 = 1.610 ns, respectively.

Generally speaking, a collision would happen between fluorophor and quencher. This kind of collision may be a dynamic collision,[44] but it may also be an optical collision[45] for the dimolecule was in the excited state. To investigate the fluorescence quenching mechanism of SiO_2@FITC-APTS@MIPs with LC, the quenching efficiency of SiO_2@FITC-APTS@MIPs was evaluated by the Stern−Volmer equation, as follows:

$$F_0/F = 1 + K_{SV}C = 1 + K_q\tau_0 C \quad (1)$$

F_0 is the initial fluorescence intensity without analyte. F is the fluorescence intensity with the concentration of analyte. K_{SV} is the Stern−Volmer quenching constant in units of L mol^{-1}. C is the concentration of molecular targets. K_q is the rate constant of the bimolecular quenching process in units of L mol^{-1} s^{-1}. τ_0 is the lifetime without quenching agent.

We did reproducibility experiments three times and acquired Figure 4 by their average. As shown in Figure 3a, LC, the concentration range of which was 0−60 nM L^{-1}, could have a good linear relationship with fluorescence intensity. The linear equation of SiO_2@FITC-APTS@MIPs was $F_0/F - 1$ = 0.0162C + 0.0272, and the corresponding correlation coefficient was R^2 = 0.9968. The limit of detection is evaluated using LOD = $3\sigma/S$ and is found to be 9.17 nM L^{-1}, where σ is the standard deviation of the blank signal and S is the slope of the linear calibration plot. From Figure 4a, we could see that the concentration range of analyte was 0−60 nM L^{-1}. From Figure 4b, we could see the linear equation of fluorescence intensity and the concentration of LC (also from 0 to 60 nM L^{-1}) was $F_0/F - 1$ = 0.0044C + 0.0081, with R^2 = 0.9947.

DOI: 10.1021/jf5043823
J. Agric. Food Chem. 2015, 63, 2392−2399

When it surpassed the range of linear concentration, the slope of quenching became gentle. When the concentration was >250 nM L^{-1}, the quenching rate almost reached saturation.

The lifetimes are quite different whether the quenching agent exists or not. We found another kind of representation of the Stern−Volmer equation according to eq 1

$$\tau_0/\tau = 1 + K_{SV}C = 1 + K_q\tau_0 C \quad (2)$$

where τ is the lifetime with quenching agent.

According to eq 2, we found the relationship $K_{SV} = K_q\tau_0$. Now we know τ_0 = 1.6102 ns, which does not exist for quenching agent, and K_{SV} = 0.0044 L mol^{-1} via the above linear equation of SiO_2@FITC-APTS@NIPs. Therefore, $K_{q(NIPs)}$ = 3.792E6 L mol^{-1} s^{-1} was calculated by the equation. $K_{q(MIPs)}$ = 1.107E7 L mol^{-1} s^{-1} by the same method. K_q is the rate constant of the bimolecular quenching process, which represents bimolecular encountering frequency orders of magnitude. The rate constant (K_q) of maximum diffusion-controlled dynamic quenching, which is between the quenching agent and fluorescent molecule, is 2.0E10 L mol^{-1} s^{-1}.[46] The K_q in this study is always <2.0E10 L mol^{-1} s^{-1}, so the reason for fluorescence quenching is dynamic quenching. Due to many specific binding sites existing in the fluorescent molecularly imprinted polymer because $K_{q(MIPs)}$ (1.107E7 L mol^{-1} s^{-1}) > $K_{q(NIPs)}$ (3.792E6 L mol^{-1} s^{-1}), the fluorescent molecularly imprinted polymer is more likely to cause the fluorescence quenching phenomenon than fluorescent molecularly non-imprinted polymer. That is to say, the fluorescent molecularly imprinted polymer is more likely to occur with bimolecular dynamic collision, thereby producing dynamic quenching. We could draw the conclusion that the molecularly imprinted polymer not only had a high quenching rate but also a wide linear range. The obtained high quenching efficiency of the SiO_2@FITC-APTS@MIPs resulted from specific recognition sites for template molecule created during the course of imprinting.

Selectivity Determination. To measure the selectivity of the SiO_2@FITC-APTS@MIPs beads further, we made a comparison between the potential interference of several structurally related compounds (BC, FE, and BI) and LC. The SiO_2@FITC-APTS@MIPs beads were added to 10 mL of ethanol solutions containing 30 nM L^{-1} of BC, FE, and BI, respectively. The mixture was stirred for 1.0 h at the room temperature. The fluorescence intensity was detected by the fluorescence spectrophotometer, and $[(F_0/F) - 1]$ was calculated with the fluorescent data.

As shown in Figure S8a in the Supporting Information, the fluorescence quenching intensity of SiO_2@FITC-APTS@MIPs for LC was much lower than that of the structural analogues. It showed that only LC could adapt to the recognition sites in SiO_2@FITC-APTS@MIPs rather than other structural analogues, which could generate more fluorescence quenching efficiency. However, SiO_2@FITC-APTS@NIPs had a lower fluorescence quenching rate than the imprinting in Figure S8b. Other structural analogues were the same as LC, and their fluorescence quenching rates were all low. In conclusion, the fluorescence quenching of SiO_2@FITC-APTS@NIPs was invisible, because there were nonspecific recognition sites in SiO_2@FITC-APTS@NIPs.

As shown in Figure 5, the chemical structures of each structural analogue are displayed. We could see from Figure 5 that the fluorescence quenching efficiency of SiO_2@FITC-APTS@MIPs for LC was much higher than that of other

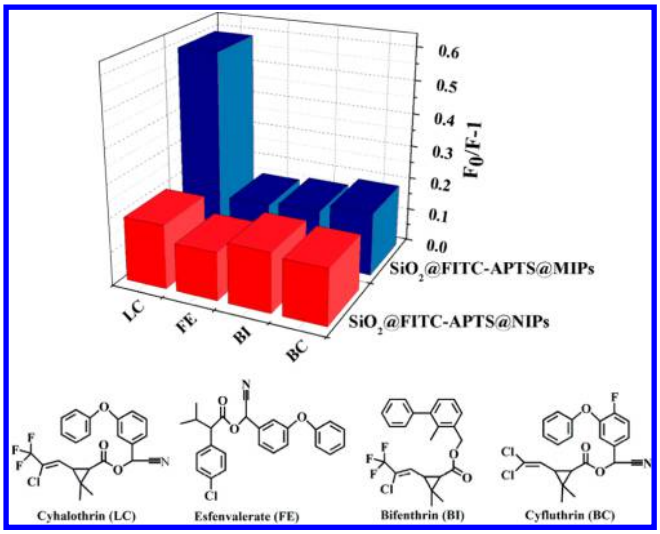

Figure 5. Quenching amount of SiO_2@FITC-APTS@MIPs and NIPs by different kinds of 30 nM L^{-1} pyrethroid pesticides and the chemical structures of each pyrethroid pesticide.

structural analogues. The results showed that SiO_2@FITC-APTS@MIPs had good selectivity for λ-cyhalothrin and none of the competitors being evaluated led to any significant fluorescence quenching rate. It can be proved that the SiO_2@FITC-APTS@MIPs beads provided high selectivity for LC, which was produced for the reason that there were specific recognition sites of LC in SiO_2@FITC-APTS@MIPs.

To further the investigation of how the competitive analogue affects the fluorescence quenching, BC, FE, and BI, these three competitive pesticides, were added into LC solution to form blend solutions, and the concentrations of λ-cyhalothrin and the competitive pesticides were all 30 nM L^{-1}. As can be seen from Figure 6, these three competitive pesticides could not obviously interfere with the fluorescence intensity of SiO_2@FITC-APTS@MIPs and NIPs. As can be seen from Figure 6a, the addition of structural analogues had almost no effect on the detection of LC. The last complex sample (LC, BC, BI, and FE) had too many structural analogues, so the SiO_2@FITC-APTS@MIPs could not detect the LC very well. The SiO_2@FITC-APTS@NIPs may be for the same reason in Figure 6b. From what had been discussed above, we could draw the conclusion that the SiO_2@FITC-APTS@MIPs provided high selectivity for LC, and it had good anti-interference for structural analogues. That is to say, the product of SiO_2@FITC-APTS@MIPs can identify the target molecule from the complex samples very well.

Application to Water Sample Analysis. To assess the applicability of SiO_2@FITC-APTS@MIPs beads in three water samples, we collected the distilled water and tap water from the laboratory, and we bought the Chinese spirits from a supermarket in China. We selected four concentrations to evaluate the applicability of SiO_2@FITC-APTS@MIPs beads and got the recovery by parallel measurement five times. The 5.0 mL water sample was added into 5.0 mL of LC solution (0−500 nM L^{-1}) and analyzed by the procedure mentioned above. Table 2 lists the corresponding results. The results showed that the SiO_2@FITC-APTS@MIPs had a good recovery in the linear concentration range, regardless of whether it was water sample or Chinese spirits. The recovery is smaller and smaller beyond the linear concentration range. The Chinese spirit sample is relatively complex, but it still has a

DOI: 10.1021/jf5043823
J. Agric. Food Chem. 2015, 63, 2392−2399

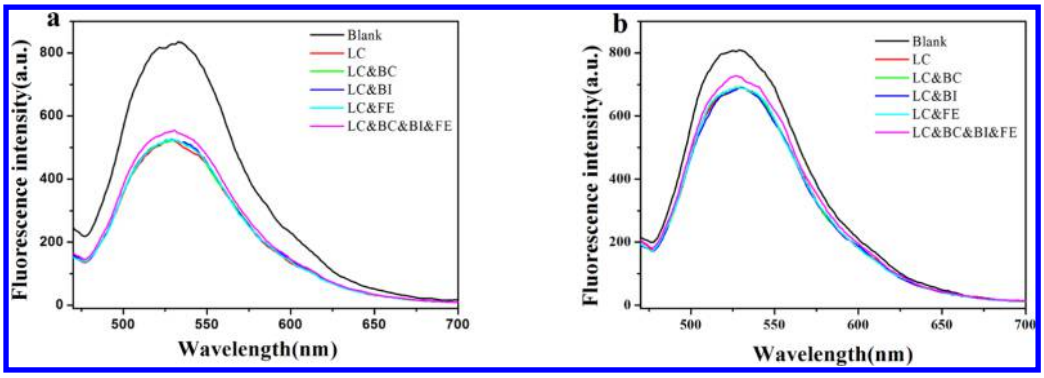

Figure 6. Quenching amount of SiO_2@FITC-APTS@MIPs (a) and SiO_2@FITC-APTS@NIPs (b) by different kinds of 30 nM L^{-1} pyrethroid pesticides.

Table 2. Recovery of LC-Spiked Water Samples Using the Proposed Sensor

sample	test	LC added (nM)	LC found[a] (nM)	recovery (%)
distilled water	1	0	0	
	2	8	7.9 ± 0.2	98.8 ± 2.5
	3	60	60.5 ± 0.9	100.8 ± 1.5
	4	500	386 ± 2.8	77.2 ± 0.56
tap water	1	0	0.1 ± 0.1	
	2	8	8.3 ± 0.4	103.8 ± 5.0
	3	60	61.4 ± 1.2	102.3 ± 2.0
	4	500	371 ± 3.9	74.2 ± 0.78
Chinese spirits	1	0	0.2 ± 0.1	
	2	8	8.5 ± 0.5	106.2 ± 6.2
	3	60	62.8 ± 2.9	104.6 ± 4.8
	4	500	307 ± 5.1	61.4 ± 1.0

[a]Average of five measurements.

good recovery. This suggests that the SiO_2@FITC-APTS@MIPs could analyze LC in Chinese spirit samples. The results clearly establish that the SiO_2@FITC-APTS@MIPs can attain good recovery and can be effectively applied in the detection of LC in Chinese spirits.

To appraise the detection for SiO_2@FITC-APTS@MIPs beads with interferences further, we selected a better recovery of concentration (60 nM L^{-1}) to assess the applicability of SiO_2@FITC-APTS@MIPs. The Chinese spirit sample 5.0 mL was added into 5.0 mL of LC solution (60 nM L^{-1}) and analyzed according to the procedure mentioned above. The recovery of the Chinese spirit sample was obtained by carrying out parallel measurements five times. Table 3 lists the corresponding results. As shown, all recoveries were >100%. The existence of error is allowed. The concentration of the

Table 3. Interferences in LC Detection in Chinese Spirits

	LC added (nM)					
test	LC	BC	BI	FE	LC found[a] (nM)	recovery (%)
1	60	0	0	0	62.1 ± 0.6	103.5 ± 1.0
2	60	60	0	0	63.3 ± 0.5	105.5 ± 0.8
3	60	0	60	0	63.2 ± 0.6	105.3 ± 1.0
4	60	0	0	60	63.4 ± 0.4	105.7 ± 0.7
5	60	60	60	60	64.2 ± 0.8	107 ± 1.3

[a]Average of five measurements.

fluorescent molecularly imprinted polymers in 60 nM L^{-1} is the maximum detectable concentration in the linear interval area. At the same time, the fluorescence quenching is the strongest. First, there are acids, aldehydes, ketones, aldehydes, aromatics, and other compounds in Chinese spirits. The feeble fluorescence quenching of the fluorescent molecularly imprinted polymers was caused by certain compounds in the Chinese spirits, thus resulting in the recovery becoming larger. Because the chemical structures of other competitive pyrethroids are similar to that of the target molecule, these other competitive pyrethroids also can produce certain fluorescence quenching of fluorescent molecularly imprinted polymer. However, it is not the main reason for the fluorescence quenching. Therefore, we found that the recovery would become larger with the increasing kinds of pyrethroid. On the whole, the results showed that the recovery has almost no change with single distracters. Although the recovery of the last test with three distractors is not as good as before, it still has relatively stable recovery. On the whole, the SiO_2@FITC-APTS@MIPs can attain satisfactory recovery in complex Chinese spirits.

To appraise the regeneration for SiO_2@FITC-APTS@MIPs beads, 60 nM L^{-1} LC solutions were first prepared. One hundred milligrams of SiO_2@FITC-APTS@MIPs beads was added into 100 mL of LC solution and incubated for 2.0 h before fluorescence measurement. After the test, the SiO_2@FITC-APTS@MIPs beads containing LC were washed with methanol−acetic acid solution, collected by centrifuge, and rinsed with ethanol. As shown in Figure S9 in the Supporting Information, the SiO_2@FITC-APTS@MIPs beads have certified that they can be reused five times without remarkable loss of signal intensity.

Conclusion. In summary, by combining a surface imprinting technique and fluorescent polymers, core−shell submicrometer SiO_2@FITC-APTS@MIPs on the surface of SiO_2 beads, which can be applied to the selective detection of LC, were synthesized. The unique aspects of SiO_2@FITC-APTS@MIPs, such as molecular recognition, fast separation, and fluorescence detection of target molecule were realized and discussed in detail. The adsorption of LC was detected by fluorescence spectrophotometer, and, using the Stern−Volmer equation, analyzed for fluorescence intensity. It is noteworthy that the SiO_2@FITC-APTS@MIPs not only have fluorescence property but also have quick detection, high fluorescence intensity, and good selective recognition for the target molecule. The experimental results showed the fluorescence quenching efficiency of SiO_2@FITC-APTS@MIPs for LC was

DOI: 10.1021/jf5043823
J. Agric. Food Chem. 2015, 63, 2392−2399

much higher than that of the structurally analogous composite and the SiO_2@FITC-APTS@NIPs, and it illustrated that the adsorption capacity and selectivity of the SiO_2@FITC-APTS@MIPs for the target molecule were good. From the SiO_2@FITC-APTS@MIPs detected LC in Chinese spirit samples, it can be seen that the SiO_2@FITC-APTS@MIPs not only has the advantage of high selectivity of molecular imprinting technique but also has the advantage of high sensitivity. On the whole, the present studies not only provide a new way to actualize selectively fluorescent detection of pyrethroid pesticides but also improve the potential application of molecularly imprinted polymers in the analysis field.

■ ASSOCIATED CONTENT

Supporting Information

Detailed experimental characterization for polymers such as the fluorescent equation, measurements, and additional figures (FT-IR, UV−vis spectra, CLSM images, thermal gravity analysis, results of competitive and regenerative experiments). This material is available free of charge via the Internet at http://pubs.acs.org.

■ AUTHOR INFORMATION

Corresponding Author

*(Y.Y.) Phone: +86 0511 88791800. E-mail: yys@mail.ujs.edu.cn.

Funding

This work was financially supported by the National Natural Science Foundation of China (No. 21107037, 21176107, 21407064, 21407057, 21277063, and 21346004), the Natural Science Foundation of Jiangsu Province (No. BK2011461 and BK2011514), the National Postdoctoral Science Foundation (No. 2013M530240), the Postdoctoral Science Foundation funded Project of Jiangsu Province (No. 1202002B), Programs of Senior Talent Foundation of Jiangsu University (No. 12JDG090), and Ph.D. Innovation Programs Foundation of Jiangsu Province (No. CXZZ13_0681).

Notes

The authors declare no competing financial interest.

■ REFERENCES

(1) Seenivasan, S.; Muraleedharan, N. N. *Food Chem. Toxicol.* **2009**, *47*, 502−505.
(2) Gong, J. L.; Gong, F. C.; Kuang, Y.; Zeng, G. M.; Shen, G. L.; Yu, R. Q. *Anal. Bioanal. Chem.* **2004**, *379*, 302−307.
(3) Bradberry, S. M.; Cage, S. A.; Proudfoot, A. T.; Vale, J. A. *Toxicol. Rev.* **2005**, *24* (2), 93−106.
(4) Guo, Y. R.; Liang, X.; Wang, Y. Y.; Liu, Y. H.; Zhu, G. N.; Gui, W. J. *J. Appl. Polym.* **2013**, *128*, 4014−4022.
(5) (a) Barro, R.; Garcia-Jares, C.; Llompart, M.; Cela, R. *J. Chromatogr. Sci.* **2006**, *44*, 430−437. (b) Reigart, J. R.; Roberts, J. R. *Recognition and Management of Pesticide Poisonings*, 5th ed.; U.S. Environment Protection Agency (EPA): Washington, DC, USA, 1999.
(6) Sicbaldi, F.; Sarra, A.; Mutti, D.; Bo, P. F. *J. Chromatogr., A* **1997**, *765*, 13−22.
(7) Lehotay, S. J.; Lightfield, A. R.; Harman-Fetcho, J. A.; Donoghue, D. J. *J. Agric. Food Chem.* **2001**, *49*, 4589−4596.
(8) Pang, G. F.; Fan, C. L.; Chao, Y. Z.; Zhao, T. S. *J. Chromatogr., A* **1994**, *667*, 348−353.
(9) Fernández-Gutiérrez, A.; Martínez-Vidal, J. L.; Arrebola, F. J.; Gonzalez-Casado, A.; Vílchez, J. L. *Fresenius' J. Anal. Chem.* **1998**, *360*, 568−572.
(10) López-López, T.; Gil-Garcia, M. D.; Martínez-Vidal, J. L.; Martínez-Galera, M. *Anal. Chim. Acta* **2001**, *447*, 101−111.
(11) Pasha, A.; Vijayashankar, Y. N. *Analyst* **1993**, *118*, 777−778.
(12) Patil, V. B.; Sevalkar, M. T.; Padalikar, S. V. *Analyst.* **1992**, *117*, 75−76.
(13) Argauer, R. J.; Eller, K. I.; Pfeil, R. M.; Brown, R. *J. Agric. Food Chem.* **1997**, *45*, 180−184.
(14) Ramesh, A.; Balasubramanian, M. *Analyst* **1998**, *123*, 1799−1802.
(15) Huang, X. H.; Zhao, X. H.; Lu, X. T.; Tian, H. P.; Xu, A. J.; Liu, Y.; Jian, Z. *J. Chromatogr., B* **2014**, *967*, 1−7.
(16) Deme, P.; Azmeera, T.; Devi, L. A. P.; Jonnalagadda, P. R.; Prasad, R. B. N.; Vijaya Sarathi, U. V. R. *Food Chem.* **2014**, *142*, 144−151.
(17) Esteve-Turrillas, F. A.; Pastor, A.; Guardia, M. D. L. *Anal. Bioanal. Chem.* **2006**, *384* (3), 801−809.
(18) Gao, D. M.; Zhang, Z. P.; Wu, M. H.; Xie, C. G.; Guan, G. J.; Wang, D. P. *J. Am. Chem. Soc.* **2007**, *129* (25), 7859−7866.
(19) Haupt, K.; Mosbach, K. *Chem. Rev.* **2000**, *100*, 2495−2504.
(20) Zimmerman, S. C.; Wendland, M. S.; Rakow, N. A.; Zharov, I.; Suslick, K. S. *Nature* **2002**, *418*, 399−403.
(21) Mertz, E.; Zimmerman, S. C. *J. Am. Chem. Soc.* **2003**, *125* (12), 3424−3425.
(22) Katz, A.; Davis, M. E. *Nature* **2000**, *403*, 286−289.
(23) Bass, J. D.; Katz, A. *Chem. Mater.* **2003**, *15* (14), 2757−2763.
(24) Xie, C. G.; Liu, B. H.; Wang, Z. Y.; Gao, D. M.; Guan, G. J.; Zhang, Z. P. *Anal. Chem.* **2008**, *80* (2), 437−443.
(25) Pan, J. M.; Yao, H.; Xu, L. C.; Ou, H. X.; Huo, P. W.; Li, X. X.; Yan, Y. S. *J. Phys. Chem. C* **2011**, *115*, 5440−5449.
(26) Xu, L. C.; Pan, J. M.; Dai, J. D.; Li, X. X.; Hang, H.; Cao, Z. J.; Yan, Y. S. *J. Hazard. Mater.* **2012**, *48*−*56*, 233−234.
(27) Jenkins, A. L.; Uy, O. M.; Murray, G. M. *Anal. Chem.* **1999**, *71* (2), 373−378.
(28) Ansell, R. J.; Mosbach, K. *Analyst* **1998**, *123* (7), 1611−1616.
(29) Levi, R.; McNiven, S.; Piletsky, S. A.; Cheong, S. H.; Yano, K.; Karube, I. *Anal. Chem.* **1997**, *69* (11), 2017−2021.
(30) Kong, X.; Gao, R. X.; He, X. W.; Chen, L. X.; Zhang, Y. K. *J. Chromatogr., A* **2012**, *1245*, 8−16.
(31) Gao, R. X.; Su, X. Q.; He, X. W.; Chen, L. X.; Zhang, Y. K. *Talanta* **2011**, *83* (3), 757−764.
(32) Gao, R. X.; Kong, X.; Su, F. H.; He, X. W.; Chen, L. X.; Zhang, Y. K. *J. Chromatogr., A* **2010**, *1217* (52), 8095−8102.
(33) Shi, X.; Liu, J.; Sun, A.; Chen, J. *J. Chromatogr., A* **2012**, *1227*, 60−66.
(34) Ma, G.; Chen, L. *J. Chromatogr. A* **2014**, *1329*, 1−9.
(35) Feng, H.; Wang, N. Y.; Trans, T. T. T.; Yuan, L. J.; Li, J. Z.; Cai, Q. Y. *Sens. Actuators, B−Chem.* **2014**, *195*, 266−273.
(36) Zhao, Y. Y.; Ma, Y. X.; Li, H.; Wang, L. Y. *Anal. Chem.* **2012**, *84*, 386−395.
(37) Song, Z. L.; Liu, C. B.; Pan, J. M.; Yan, Y. S.; Wei, X.; Meng, M. J.; Yu, P.; Gao, L.; Dai, J. D.; Lin, S. *Anal. Methods* **2014**, *6*, 915−923.
(38) Li, Y. L.; Cui, Z. M.; Li, D. P.; Li, H. B. *Sens. Actuators, B−Chem.* **2011**, *155* (2), 878−883.
(39) Stober, W.; Fink, A. *J. Colloid Interface Sci.* **1968**, *26*, 62−69.
(40) Chen, S. L.; Yuan, G. M.; Hu, C. T. *Powder Technol.* **2011**, *207* (1−3), 232−237.
(41) Imhof, A.; Megens, M.; Engelberts, J. J.; Lang de, D. T. N.; Sprik, R.; Vos, W. L. *J. Phys. Chem. B* **1999**, *103* (9), 1408−1415.
(42) Li, H. L.; Perkas, N.; Li, Q. L.; Gofer, Y.; Koltypin, Y.; Gedanken, A. *Langmuir* **2003**, *19* (24), 10409−10413.
(43) Wang, H. F.; He, Y.; Ji, T. R.; Yan, X. P. *Anal. Chem.* **2009**, *81* (4), 1615−1621.
(44) Ganter, M. A.; Uicker, J. J. *J. Mech. Des.* **1986**, *108* (4), 549−555.
(45) Coggeshall, N. D.; Saier, E. L. *J. Chem. Phys.* **2004**, *15* (1), 65−71.
(46) Ware, W. R. *J. Phys. Chem.* **1962**, *66*, 455−458.

DOI: 10.1021/jf5043823
J. Agric. Food Chem. 2015, 63, 2392−2399